Infrared Spectrum of the H_3N-HCl Complex in Solid Ne, Ne/Ar, Ar, and Kr. Matrix Effects on a Strong Hydrogen-Bonded Complex

Lester Andrews,*,† Xuefeng Wang,† and Zofia Mielke‡

Departments of Chemistry, University of Virginia, Charlottesville, Virginia 22904-4319, and University of Wroclaw, Wroclaw, PL-50383 Poland

Received: January 25, 2001; In Final Form: March 27, 2001

Ammonia and hydrogen chloride vapors from thermal decomposition of NH_4Cl co-deposited with excess neon at 4−5 K formed the H_3N-HCl complex. Strong, broad 2084 cm^{-1} and strong, sharp 1060.2 cm^{-1} absorptions are assigned to the H−Cl stretching and symmetric NH_3 bending modes and weaker 2017.4 and 708.9 cm^{-1} bands to the overtone of the NH_3 mode and the H−Cl librational fundamental of the 1:1 complex. Complementary experiments were done with neon/argon mixtures, argon, and krypton to investigate the 1:1 complex in a range of matrix environments. Vibrational assignments are supported by $^{15}NH_4Cl$, ND_4Cl, and $^{15}ND_4Cl$ isotopic substitution. The neon matrix spectrum suggests a strong hydrogen bond, slightly stronger than in the gas-phase complex, but not as strong as found in the argon and krypton matrix hosts owing to increased solvation by the more polarizable matrix atoms.

Introduction

The hydrogen-bonded complexes formed between ammonia or amines and hydrogen halides have been the subject of considerable interest.[1] A question of chemical significance concerns the nature of these complexes in the gas phase. Theoretical and experimental studies have been performed to decide whether the complexes are better described as hydrogen-bonded dimers or ion-pairs and to determine the extent of proton transfer in the particular complex.

The ammonia−hydrogen chloride complex holds a special position in these investigations as the archetypical model for the study of hydrogen bonding. Early theoretical calculations[2] stimulated the experimental attempts to characterize the complex. The H_3N-HCl complex was first detected by high-temperature mass spectrometry[3] and by gas-phase electron diffraction.[4] However, attempts to obtain infrared spectra from metastable gas-phase mixtures of ammonia and hydrogen chloride were unsuccessful because of nucleation of ammonium chloride crystals.[5] Infrared spectra were recorded for the first time for the complex isolated in a nitrogen matrix and interpreted in terms of a proton-shared hydrogen bond in which the hydrogen atom of HCl is shared by the chlorine and nitrogen atoms.[6] The infrared matrix-isolation studies of the complex isolated in solid argon demonstrated a large difference between the spectra of the complex in argon and nitrogen matrices.[7] Similar differences were also found for the amine−hydrogen chloride,[8] hydrogen bromide,[9] and hydrogen iodide[10] complexes isolated in argon and nitrogen matrices. These studies demonstrated the importance of the environment, the more strongly interacting nitrogen matrix increasing the extent of proton transfer from the hydrogen halide to the amine as compared with the complex isolated in an argon matrix.

The development of rotational spectroscopy for supersonically expanded jets allowed the structure of the ammonia−hydrogen chloride complex to be established in the gas phase.[11] The complex can be described as the simple hydrogen-bonded type, without the need to invoke an appreciable extent of proton transfer. This result agrees with several recent ab initio calculations, which indicate a simple molecular hydrogen-bonded complex with no significant proton transfer.[12−14] However, in clusters with two or more water molecules[15] and on crystalline ice,[16] NH_3 and HCl form the ion pair $NH_4^+Cl^-$. Recent DFT calculations show that the complex dimer sustains proton transfer to give a four-ion $(NH_4^+)_2(Cl^-)_2$ cluster.[17]

The extent of proton transfer in the ammonia−hydrogen chloride complex isolated in solid argon and nitrogen and estimated from the vibrational spectra is larger than that inferred from the rotational spectroscopic data.[1,18] Very recent MP2 calculations[19,20] have included anharmonicity in the H_3N-HCl potential and matrix effects to account for the low H−Cl stretching frequency observed in matrix infrared experiments. Since there is a valid question about environmental perturbations or matrix effects on the H_3N-HCl complex trapped in solid argon and nitrogen, it is desirable to obtain the spectrum in the more inert neon matrix to more closely approach gas-phase conditions. For the similar H_3N-HF complex, the neon matrix H−F mode (3106 cm^{-1}) falls intermediate between gas-phase (3215 cm^{-1}) and argon matrix (3041 cm^{-1}) values.[21−23] We report here the infrared spectrum of the H_3N-HCl complex isolated in solid neon, neon/argon, and krypton, which shows the effect of the heavier matrix hosts on the vibrational characteristics of the complex. A preliminary communication on the neon matrix spectrum has appeared.[24]

Experimental and Computational Section

Ammonia and hydrogen chloride vapors from thermal decomposition of solid NH_4Cl were co-deposited with excess neon at 3 mmol/h onto a 4−5 K (Heliplex APD Cryogenics) CsI window for two or three 30 min periods, and infrared spectra were recorded on a Nicolet 750 instrument at 0.5 cm^{-1} resolution. The solid NH_4Cl (EM Science, GR) was thoroughly degassed and heated[25] externally to 70−90 °C in a Teflon bore

* Author for correspondence.
† University of Virginia.
‡ University of Wroclaw.

10.1021/jp010323x CCC: $20.00
Published on Web 06/05/2001

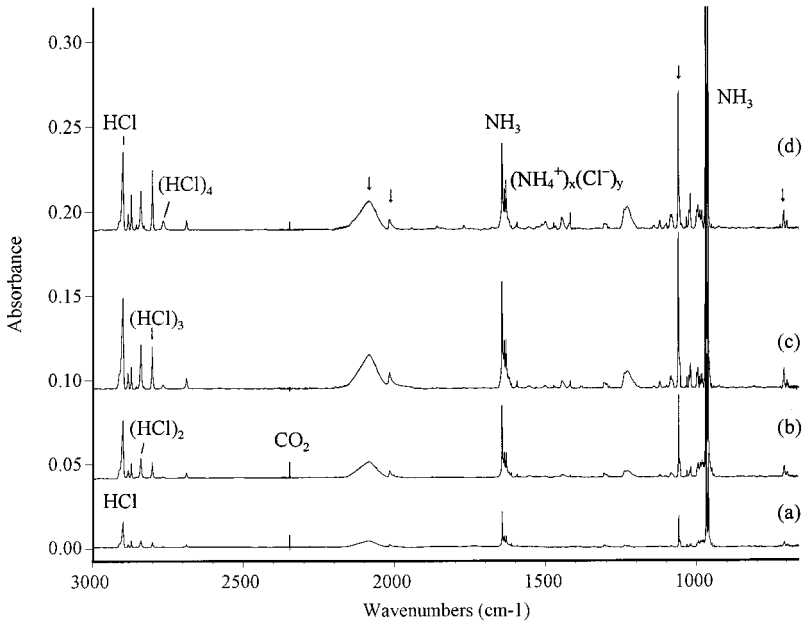

Figure 1. Infrared spectra in the 3000−700 cm^{-1} region for ammonia and hydrogen chloride vapors trapped in solid neon at 4−5 K. (a) After 30 min deposition, (b) after 60 min, (c) after 90 min, and (d) after annealing to 8 K.

right-angle valve (Ace Glass, 3 mm) controlled sample tube with 11 cm sidearm through a vacuum fitting to a point 2 cm from the cold surface. The NH_3 concentration in the neon matrix is estimated to be about 0.1% from published spectra.[26] Deuterated samples were prepared by exchanging NH_4Cl with D_2O in the sample tube and evaporating residual D_2O at 40−50 °C, which serves to exchange deuterate the sidearm and allow for the delivery of relatively pure DCl and ND_3 into the matrix. Solid $^{15}NH_4Cl$ (98% ^{15}N, Aldrich) was used directly, and $^{15}ND_4Cl$ was also prepared by exchange with D_2O.

Density functional theory (DFT) calculations[27] were used to predict frequencies for the H_3N-HCl and H_3N-HF complexes. The B3LYP and BPW91 functionals and 6-311+G** basis sets were employed.[28−30] All geometrical parameters were fully optimized, and harmonic vibrational frequencies were computed analytically at the optimized structures.

Results

Neon. Infrared spectra are shown in Figure 1 for three 30 min deposition periods and a subsequent annealing to 8 K. The spectra of NH_3, $(NH_3)_2$, HCl, $(HCl)_2$, and $(HCl)_3$ agree with previous reports;[26,31,32] note that the monomer HCl and NH_3 species dominate in each spectral region, but the population of dimer species increases with sample thickness. The dominance of HCl monomer is even more striking when the substantially increased infrared intensity of $(HCl)_2$ is considered. The strongest new features are a sharp band at 1060.2 cm^{-1} and a broad band at 2084 cm^{-1}; sharp weaker bands are found at 2017.4 and 708.9 cm^{-1} (marked with arrows (↓)). Table 1 lists all of the observed bands; no product absorption was observed in the 4400−4000 cm^{-1} region. The above band sets exhibit constant relative intensities during deposition in different experiments and decrease in concert on annealing to 8 and 10 K, while absorptions at 1086, 1230, 1418, 1446, and 3108 cm^{-1} increase. Annealing also decreases the HCl and NH_3 absorptions in favor of their dimers and trimers; note that more association is found for the smaller HCl reagent.

Experiments were also done with $^{15}NH_4Cl$ vapor co-deposited with excess neon, and the new bands (Figure 2c) appeared at 2079, 2008.4, 1054.8, and 708.9 cm^{-1} and decreased on final annealing, while bands at 1082, 1223, 1412,1440, and 3104 cm^{-1} increased.

TABLE 1: Infrared Absorptions (cm^{-1}) from Co-deposition of Ammonia and Hydrogen Chloride Vapor with Excess Neon at 4−5 K

NH_4Cl	$^{15}NH_4Cl$	ND_4Cl	$^{15}ND_4Cl$	identification
3453.0[a]	3444.6	2568.9	2557.8	NH_3, ν_3
3412.6[a]	3404.4	2541.0		$(NH_3)_2$, "ν_3"
3364.3	3361.4	2420.7		NH_3, ν_1
3319.8	3314.9	2417.7		$(NH_3)_2$, "ν_1"
3108	3104			$(NH_4^+)_x(Cl^-)_y$
2899.4	2899.4	2097.7[b]	2097.7	HCl, R(0)
2883.4	2883.4	2088.4	2088.4	X−HCl
2871.2	2871.7	2078.9[b]	2078.9	HCl, induced Q
2839.1	2839.1	2054.5[b]	2054.5	$(HCl)_2$
2801.3	2801.3	2028.0[b]	2028.0	$(HCl)_3$
2766.7	2766.7	2003.0	2003.0	$(HCl)_4$
2687.7	2687.7	1951.5, 1948.7	1951.5, 1948.7	H_2O-HCl
2084	2079	1600	1595	H_3N-HCl
2017.4	2008.4	1595	1583	H_3N-HCl
1771.1	1765.2			$(NH_4^+)_x(Cl^-)_y$
1644.7	1641.4	1199.9	1196.3	NH_3, ν_4
1445.8	1440.2	1102		$(NH_4^+)_x(Cl^-)_y$
1418.0	1412.0			$(NH_4^+)_x(Cl^-)_y$
1230	1223	996		$(NH_3)(HCl)_2$
1086.1	1081.7	847.2		$(NH_3)(HCl)_2$
1060.2	1054.8	824.5	817.1	H_3N-HCl
1031.6	1026.5	802.3	796.1	NH_3-H_2O
1019.4	1014.7	793.1	786.3	$(NH_3)_3$
994.0	989.4	779.6	773.1	$(NH_3)_2$
968.2	964.1	767.4	760.9	NH_3, ν_2
960.7	956.6	757.0	750.5	NH_3, ν_2 site
708.9	708.9	526.1	526.1	H_3N-HCl
698.3	698.3	519.1		H_3N-HCl

[a] Different site stronger than in ref 31. [b] Listed bands are $D^{35}Cl$; the resolved $D^{37}Cl$ components are 2094.7, 2075.9, 2051.6, and 2026.2 cm^{-1}, respectively.

Several investigations were done with ND_4Cl, and the best spectrum is shown at the top of Figure 2. The spectra of DCl species are in excellent agreement with previous experiments, and the spectrum of ND_3 in neon is appropriate by comparison to the spectra of ND_3 in argon and NH_3 in neon.[31] The broad, new band centered at approximately 1600 cm^{-1} exhibits a Fermi resonance (FR) window[33] at 1595 cm^{-1}, the strong, sharp

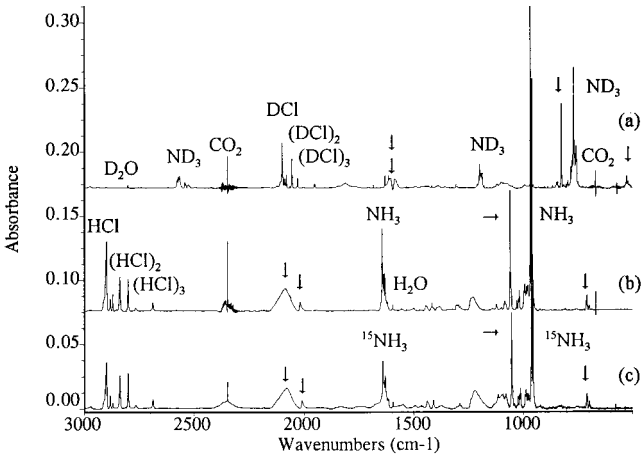

Figure 2. Infrared spectra in the 3000−500 cm^{-1} region for ammonia and hydrogen chloride vapors trapped in solid neon at 4−5 K. (a) ND_4Cl, (b) NH_4Cl, and (c) $^{15}NH_4Cl$.

absorption shifted to 824.5 cm^{-1}, and the low-frequency peak shifted to 526.1 cm^{-1}. Annealing decreased these features in favor of bands at 847.2, 996, and 1101.8 cm^{-1}. Experiments with $^{15}ND_4Cl$ provided further isotopic shifts: the broad band and Fermi resonance window shifted to 1595 and 1583 cm^{-1}, respectively, as illustrated in Figure 3, where the water bands serve as an internal calibration, and the 824.5 cm^{-1} absorption decreased to 817.1 cm^{-1}, but the 526.1 cm^{-1} band did not change. Finally, one experiment was done with almost as much $^{15}NH_4Cl$ added to the $^{15}ND_4Cl$ sample, and the resulting spectra contained about twice as much D as H species absorption. In addition to the quartet of $^{15}NH_nD_{3-n}$ symmetric bending modes from exchange of $^{15}NH_3$ and $^{15}ND_3$ in the system (including $^{15}NH_2D$ at 901.0 cm^{-1} and $^{15}NHD_2$ at 834.4 cm^{-1}), we observed a quartet of product bands at 1054.2, 954.8, 896.0, and 817.1 cm^{-1} with splittings of 0.6−1.3 cm^{-1} owing to both HCl and DCl in the reaction mixture. A broad band with center near 1595 cm^{-1} and weak FR window at 1581 cm^{-1} and another broad band with center near 2040 cm^{-1} were also observed.

Neon/Argon. A series of experiments was done with NH_4Cl, adding argon to the neon matrix gas using between 1% and 99% argon. With 1% Ar, the major absorptions are 2076 and 1060.2 cm^{-1}, and annealing to 6, 8, and 10 K shifts these peaks to 2061 and 1060.4 cm^{-1}. With 5% Ar, the major absorptions are 2045 cm^{-1}, with a FR window at 2025 cm^{-1}, and 1060.7 cm^{-1}, and annealing to 8, 10, and 12 K shifts these peaks to 2015, 1970, 1935 cm^{-1} and 1063.0, 1065.8, 1067.3 cm^{-1}, respectively. Also, the broad, upper band is tuned through the Fermi resonance window, and broad bands appear at 1420 and 1300 cm^{-1}, as shown in Figure 4. With 10% Ar, the first 30 min deposition yielded both 1061 and 1069 cm^{-1} peaks; after 60 min, the 1069.3 cm^{-1} peak dominated, and weak 2026 cm^{-1} window and broad bands at 1920, 1385, and 1295 cm^{-1} appeared; the broad 1920 cm^{-1} absorption was accompanied by a weak band at 2015 cm^{-1}. With 25% Ar, the major absorptions are 1910, 1372, 1293, and 1070 cm^{-1}. The weak 708.9 cm^{-1} band in neon is not observed with added argon, but the 734 cm^{-1} counterpart appears with 80% argon. With 80% Ar, we observed 1371, 1290, 1070, and 734 cm^{-1} bands that grow five times on annealing to 30 K (Figure 4), and then decrease on further annealing. The latter bands were also recorded using 90, 95, 98, and 100% Ar matrix samples and agree with bands observed earlier in solid argon.[7,34]

Isotopic investigations were also done with 5% argon in neon hosts. For $^{15}NH_4Cl$, the broad band shifted to 2040 cm^{-1}; the FR window was replaced by a side peak at 2007 cm^{-1}, and the strong band shifted to 1055.4 cm^{-1} with much the same appearance as Figure 4a. Stepwise annealing to 10 K shifted the broad band below the sideband to about 1930 cm^{-1}, decreased the sideband intensity, and blue-shifted the strong band to 1059.1 cm^{-1}. For ND_4Cl, the broad band shifted to 1570 cm^{-1}, clearly below the FR window at 1596 cm^{-1}, and the strong band to 825.1 cm^{-1}; stepwise annealing to 10 K shifted the broad band to 1540 cm^{-1} and blue-shifted the strong band to 826.5 cm^{-1}.

Argon. Several experiments were done with 100% argon. First, deposition at 4−5 K gave only the 2887.7, 2871.0 cm^{-1} HCl monomer, 974.7 cm^{-1} NH_3 monomer, and sharp 1070.0 cm^{-1} absorptions, but annealing to 30 K produced the same bands with half the absorbance as the 90% Ar + 10% Ne sample along with weak HCl and NH_3 dimer and trimer absorptions.[21,31,35] Second, argon was co-deposited at 8−9 K with NH_4Cl vapor, and the major product features were observed at 3429.9, 1370.9, 1290.3, 1070.0, and 733.8 cm^{-1}; annealing in a similar experiment with $^{15}NH_4Cl$ shifted the bands to 3421.7, 1364.3, 1290.1, and 1064.4 cm^{-1} and left the 733.8 cm^{-1} band unchanged. Our ND_4Cl sample produced new bands at 2553.6, 1114.3, 991.8, 831.4, and 544 cm^{-1} without the complication of NHD_2 contamination, and $^{15}ND_4Cl$ shifted these bands as listed in Table 2. Figure 5 compares selected argon matrix spectra.

Krypton. Experiments were done using krypton with 10% neon added and each ammonium chloride isotopic modification. This host condensed more transparently at 4−5 K than pure krypton, and annealing stepwise to 22, 30, and 40 K allowed the neon to escape and provided channels for more growth on annealing of the product features at 1388.5, 1281.3, 1272.4, 1218.6, 1071.8, and 736.9 cm^{-1}. Figure 6 illustrates the resulting krypton matrix spectra. Note the slight (0−3 cm^{-1}) changes in the positions of the 1281.3, 1218.6, and 1071.9 cm^{-1} bands on annealing as the neon evaporates. Further annealing to 50 K reduced the above product absorptions by 60% but did not change the frequency positions. An experiment with pure Kr on a 9−10 K substrate gave the same product yield and frequencies as annealing the Kr + 10% Ne sample to 40 K. Even on annealing to 50 K, the pure Kr sample gave no product growth. The $^{15}NH_4Cl$, ND_4Cl, and $^{15}ND_4Cl$ spectra after annealing to 38 K are also shown in Figure 6, and the isotopic absorptions after annealing are listed in Table 3.

Nitrogen. Five nitrogen matrix experiments were performed with ammonium chloride vapor to obtain new ^{15}N shift data, and the absorptions are listed in Table 4. The precursor bands agree with previous reports:[26,31,35] the 5 K nitrogen matrix trapped most of the precursor as NH_3 and HCl monomers as much weaker $(NH_3)_2$ and $(HCl)_2$ bands were observed. Spectra from $^{14}NH_4Cl$ experiments revealed bands near 3419, 1440, 1250, 702, and 628 cm^{-1}, in agreement with the early results,[6,7] but our bands are sharper using lower concentrations. Figure 7 illustrates spectra for the most informative experiment using $^{15}NH_4Cl$: annealing to 25 K sharpens the 3411.4, 1438.4, 1245.5, 700, and 625 cm^{-1} absorptions with slight growth, but $(NH_3)_2$, $(HCl)_2$, 1408.2, 1100.9, and 745.4 cm^{-1} bands clearly increase, and weak, broad 3135 and 3051 cm^{-1} bands are observed. Further annealing to 32 and 36 K produced substantial growth in 3135.4, 3051.6, and 1398.7 cm^{-1} bands, while the 745.4 cm^{-1} band remained, and the 3411.4, 1438.4, 1245.5, 700, and 625 cm^{-1} bands decreased. Final annealing to 38 K removed most of the matrix gas, reduced the latter five bands more than the 1100.9 and 745.4 cm^{-1} absorptions, and decreased the

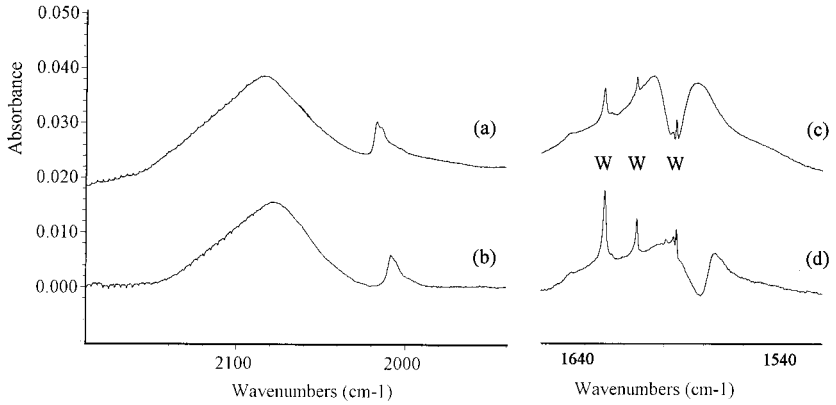

Figure 3. Broad fundamental and sharp overtone bands in Fermi resonance. (a) NH_4Cl, (b) $^{15}NH_4Cl$, (c) ND_4Cl, and (d) $^{15}ND_4Cl$. The water bands noted W at 1630.5, 1614.1, and 1594.2 cm^{-1} serve as an internal frequency standards.

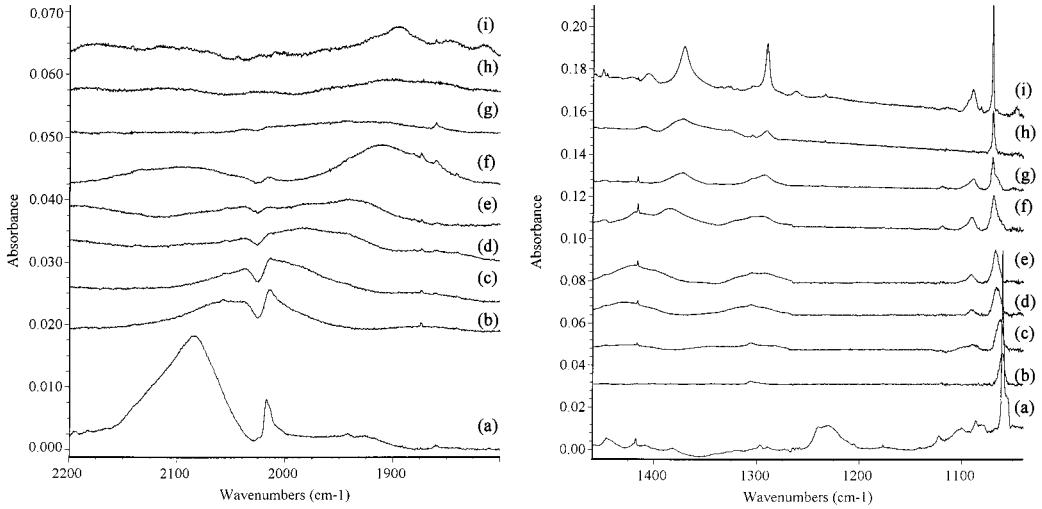

Figure 4. Infrared spectra in 2200−1800 and 1460−1040 cm^{-1} regions for NH_4Cl vapors co-deposited with mixed neon/argon samples at 4−5 K. (a) Pure neon after deposition for 90 min, (b) neon with 5% argon after deposition for 120 min, (c) after annealing to 8 K, (d) after annealing to 10 K, (e) after annealing to 12 K, (f) neon with 10% argon after deposition for 70 min, (g) neon with 25% argon after deposition for 60 min, (h) neon (20%) and argon (80%) after deposition for 60 min, and (i) after annealing to 30 K.

1398.7, 3135.4, and 3051.6 cm^{-1} features. Spectra after deposition and 36 K annealing for $^{14}NH_4Cl$ and $^{15}NH_4Cl$ samples were compared, and careful isotopic shift measurements were made for band centers.

Deuterium. One experiment was performed co-depositing NH_4Cl with D_2 gas at 4−5 K. The spectrum contained nonrotating HCl at 2868.2 cm^{-1}, a weak $(HCl)_2$ band at 2820.0 cm^{-1}, NH_3 bands at 3437.3, 3328.1, 1633.4, and 982.0 cm^{-1}, and a broad 1054 cm^{-1} product absorption. Annealing to 6.8 K had no effect, but annealing to 7.5 K sublimed some D_2 matrix, and the only absorptions remaining were broad 3066 and 1404 cm^{-1} ammonium chloride features.[36]

Calculations. The structures and harmonic frequencies computed for HCl, HF, and the H_3N-HCl and H_3N-HF complexes in C_{3v} symmetry are given in Table 5 for the B3LYP and BPW91 density functionals. The calculated HCl bond lengths are 0.005 and 0.012 Å longer, respectively, and the HF distances are 0.005 and 0.012 Å longer than experimental values.[37] However, the calculated N···Cl lengths are 0.063 and 0.117 Å shorter, respectively, than the 3.137 Å N···Cl distance for the gaseous complex.[11] The bond lengths calculated here are in ±0.01 Å agreement with B3LYP values using different basis sets.[17] Similarly, the calculated N···F lengths are 0.02 and 0.04 Å shorter than the 2.66 Å gas-phase distance[38] for H_3N-HF, and the B3LYP H−F frequency (3260 cm^{-1}) is slightly higher than the gas-phase value (3215 cm^{-1}),[22] while

TABLE 2: Infrared Absorptions (cm^{-1}) from Co-deposition of Ammonia and Hydrogen Chloride Vapor with Excess Argon at 8−9 K

NH_4Cl	$^{15}NH_4Cl$	ND_4Cl	$^{15}ND_4Cl$	identification
3447.0	3439.0	2556	2544	NH_3, ν_3
3429.9	3421.7	2553.6	2541.4	H_3N-HCl
3400.3	3392.1	2527.2	2515.3	$(NH_3)_2$, "ν_3"
3344.8	3342.0			NH_3, ν_1
3310.3	3306.4			$(NH_3)_2$, "ν_1"
2887.7	2887.7	2089.3	2089.3	HCl, R(0)
2871.6	2871.6	2079.2	2079.2	HCl, induced Q
2817.4	2817.4	2038.8	2038.8	$(HCl)_2$
2786.7	2786.7	2017.5	2017.5	$(HCl)_3$
2747.4	2747.4	1995.0	1995.0	$(HCl)_4$
2664.2	2664.2	1930.2	1930.2	H_2O-HCl
1638.5	1635.3	1190.8	1187.2	NH_3, ν_4
1449.9	1444.3			$(NH_4^+)_x(Cl^-)_y$
1446.3	1440.5	1067	1061	$(NH_4^+)_x(Cl^-)_y$
1416.2	1410.4			$(NH_4^+)_x(Cl^-)_y$
1370.9	1364.3	1114.3	1111.0	H_3N-HCl
1290.3	1290.1	991.8	989.8	H_3N-HCl
		909.9	903.0	D_3N-DCl
1089.2	1084.1	844.4	837.4	$(NH_3)(HCl)_2$
1070.0	1064.4	831.4	823.7	H_3N-HCl
1035.0	1029.9	805.1	798.1	H_3N-H_2O
1018.0	1013.4	791.7	785.3	$(NH_3)_3$
999.9	995.3	780.4	773.9	$(NH_3)_2$
974.6	970.5	759.7	752.9	NH_3, ν_2
733.8	733.8	544.0	544	H_3N-HCl
730.3	730.3			H_3N-HCl

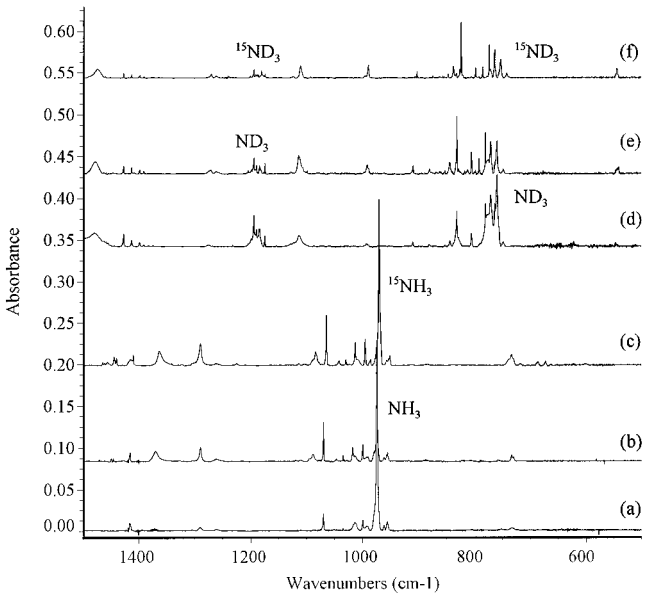

Figure 5. Infrared spectra in the 1450−500 cm^{-1} region for NH_4Cl vapors co-deposited with excess argon at 8−9 K. (a) NH_4Cl vapors deposited for 60 min, (b) after annealing to 30 K, (c) $^{15}NH_4Cl$ deposited and annealed to 30 K, (d) ND_4Cl deposited for 60 min, (e) after annealing to 30 K, and (f) $^{15}ND_4Cl$ deposited and annealed to 30 K.

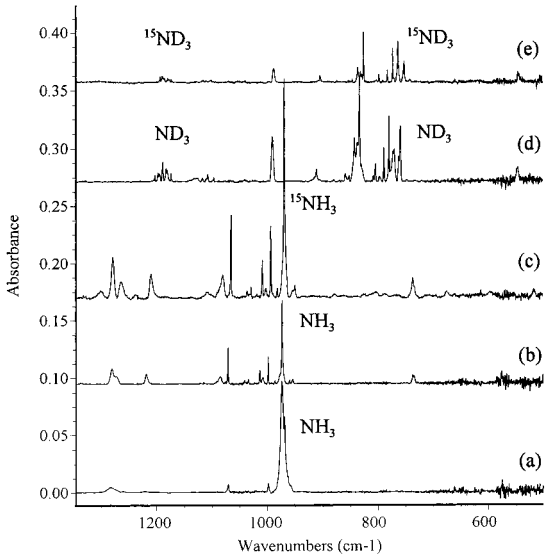

Figure 6. Infrared spectra in the 1350−500 cm^{-1} region for NH_4Cl vapors co-deposited with excess krypton with 10% neon at 4−5 K. (a) NH_4Cl vapors deposited for 60 min, (b) after annealing to 40 K, (c) $^{15}NH_4Cl$ vapors deposited and annealed to 38 K, (d) ND_4Cl vapors deposited and annealed to 38 K, and (e) $^{15}NH_4Cl$ vapors deposited and annealed to 38 K.

the BPW91 result (3023 cm^{-1}) is slightly lower. Hence, the B3LYP frequencies may have predictive value. The influence of successively fixed, shorter hydrogen bond lengths on the optimized frequencies was explored in order to simulate the effect of matrix solvation, and these approximate results are summarized in Table 6.

Discussion

The neon matrix absorptions will be assigned to the 1:1 H_3N-HCl complex, and the effect of different matrix environments on this strong hydrogen-bonded complex will be considered.

Neon. The new 2084, 2017.4, 1060.2, and 708.9 cm^{-1} absorptions track together during sample deposition in all experiments, and they decrease on final annealing, while

TABLE 3: Infrared Absorptions (cm^{-1}) from Co-deposition of Ammonia and Hydrogen Chloride Vapor with Excess Krypton Containing 10% Neon at 4−5 K[a]

NH_4Cl	$^{15}NH_4Cl$	ND_4Cl	$^{15}ND_4Cl$	identification
3434.5	3426.5	2551.0	2539.5	NH_3, ν_3
3419.9	3411.5	2546.5	2534.3	H_3N-HCl
3393.4	3385.3	2522.8	2511.1	$(NH_3)_2$, "ν_3"
3335	3332			NH_3, ν_1
2872.7	2872.7	2078.8	2078.8	HCl, R(0)
2852.8	2852.8	2068.4	2068.4	HCl, induced Q
2815.1	2815.1	2037.2	2037.2	$(HCl)_2$
2789.5	2789.5	2019.5	2019.5	$(HCl)_3$
2758.2	2758.2	1999.4	1999.4	$(HCl)_4$
1635.7	1632.5	1188.7	1185.1	NH_3, ν_4
1455.2	1450.2	1117.8	1110.7	$(NH_4^+)_x(Cl^-)_y$
1415.2	1409.4	1108.1	1102.1	$(NH_4^+)_x(Cl^-)_y$
1388.5	1379.4			$(NH_3)_x(HCl)_y$
1281.3	1279.7	991.4	988.9	H_3N-HCl
1272.4	1266.5	broad	broad	H_3N-HCl
1218.6	1210.3	911.4	904.6	H_3N-HCl
1086.3	1080.8	842.3	836.2	$(NH_3)(HCl)_2$
1071.9	1066.1	833.1	825.2	H_3N-HCl
1034.6	1029.3	804.0	797.7	H_2O-HCl
1013.7	1009.0	788.0	782.4	$(NH_3)_3$
998.3	993.7	779.4	772.9	$(NH_3)_2$
974.0	969.8	759.0	752.2	NH_3, ν_2
736.9	736.9	546.7	546.7	H_3N-HCl
734.0	734.0			H_3N-HCl

[a] The 1388.5, 1281.3, 1272.4, 1218.6, 1071.9, and 736.9 cm^{-1} bands and isotopic counterparts reported after 38−40 K annealing to remove neon and allow diffusion.

TABLE 4: Infrared Absorptions (cm^{-1}) from Co-deposition of Ammonia and Hydrogen Chloride Vapor with Excess Nitrogen at 5 K

NH_4Cl	$^{15}NH_4Cl$	identification
3440.7	3432.5	NH_3, ν_3
3419.7	3411.4	H_3N-HCl
3401.3	3393.8	$(NH_3)_2$, "ν_3"
3330.4	3327.6	NH_3, ν_1
3311.8	3307.7	$(NH_3)_2$, "ν_1"
3141.7	3135.4	$NH_4^+Cl^-$
3058.0	3051.6	$NH_4^+Cl^-$
2854.3	2854.3	HCl
2815.7	2815.7	$(HCl)_2$
2568.8	2561.6	$(NH_3)_x(HCl)_y$
1794.9	1788.5	$NH_4^+Cl^-$
1630.6	1627.5	NH_3, ν_4
1454.0	1447.8	H_3N-HCl
1443.9	1438.4	H_3N-HCl
1415.0	1408.2	$(NH_4^+)_x(Cl^-)_y$
1405.0	1398.7	$NH_4^+Cl^-$
1251.6	1245.5	H_3N-HCl
1144.4	1139.1	NH_3, $\nu_2+\nu_{lib}$
1115.8	1110.7	$(NH_3)(HCl)_2$
1106.0	1100.9	$(NH_3)(HCl)_2$
1003.4	998.9	$(NH_3)_2$
985.5	981.3	$(NH_3)_2$
969.6	965.2	NH_3, ν_2
750.4	745.7	$(NH_3)_x(HCl)_y$
702	700	H_3N-HCl
628	625	H_3N-HCl

absorptions at 3108, 1446, 1418, 1230, and 1086 cm^{-1} increase. The former three bands are in the regions of the ν_3 and ν_4 modes of solid ammonium chloride[36] and are near residual absorptions on the window after matrix evaporation. The 1086.1 cm^{-1} band shows the isotopic shifts for a symmetric NH_3 mode, and its larger displacement from ammonia than the strong 1060.2 cm^{-1} primary product band indicates a stronger interaction like that expected for the 1:2 complex $H_3N-(HCl)_2$; an associated 1230 cm^{-1} band is appropriate for the more strongly bonded H−Cl stretching mode in this 1:2 complex. The latter higher complex

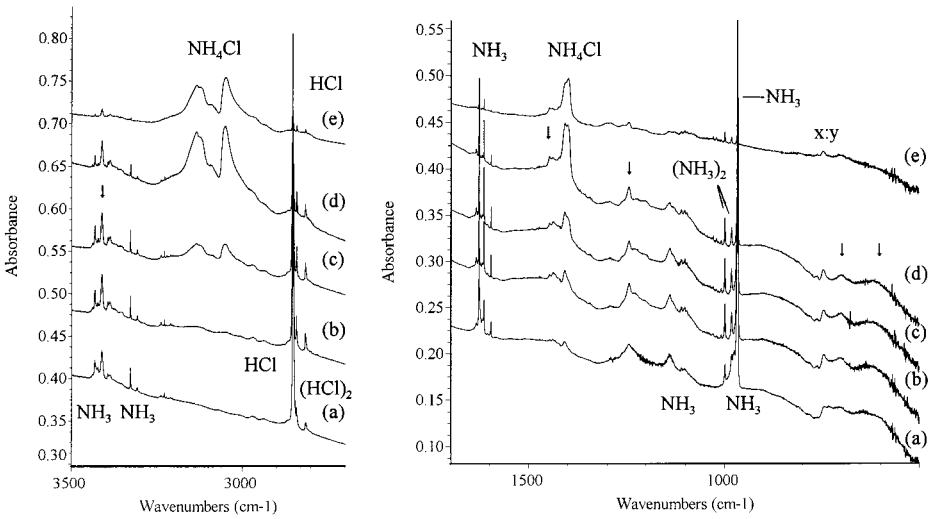

Figure 7. Infrared spectra in the 3500−2700 and 1700−500 cm^{-1} regions for $^{15}NH_4Cl$ vapors trapped in solid nitrogen at 5 K. (a) After 60 min deposition, (b) after annealing to 25 K, (c) after annealing to 32 K, (d) after annealing to 36 K, and (e) after annealing to 38 K.

TABLE 5: Frequencies (cm^{-1}), Intensities (km/mol), and Bond Lengths (Å) Calculated for the H_3N-HCl and H_3N-HF Complexes in C_{3v} Symmetry Using Density Functional Theory

H_3N-HCl[a]	B3LYP/6-311+G**
H−N: 1.016	3594 (e, 19), 3474 (a_1, 1), 2123 (a_1, 2242), 1662 (e, 27)
N−H: 1.724	1121 (a_1, 129), 855 (e, 62), 273 (e, 16), 195 (a_1, 40)
H−Cl: 1.351	
H_3N-HCl[b]	BPW91/6-311+G**
H−N: 1.022	3531 (e, 20), 3405 (a_1, 1), 1901 (a_1, 2656), 1622 (e, 265)
N−H: 1.642	1100 (a_1, 84), 922 (e, 53), 288 (e, 15), 214 (a_1, 57)
H−Cl: 1.378	
H_3N-HF[c]	B3LYP/6-311+G**
H−N: 1.016	3596 (e, 18), 3480 (a_1, 1) 3260 (a_1, 1740), 1664 (e, 23)
N−H: 1.677	1138 (a_1, 169), 1009 (e, 173), 283 (e, 8), 276 (a_1, 8)
H−F: 0.961	
H_3N-HF[d]	BPW91/6-311+G**
H−N: 1.022	3527 (e, 16), 3408 (a_1, 1), 3023 (a_1, 1863), 1627 (e, 22)
N−H: 1.641	1124 (a_1, 140), 1035 (a_1, 157), 294 (e, 9), 286 (a_1, 10)
H−F: 0.977	

[a] Angle HN−H: 110.9°, dipole moment 5.05 D. Compare HCl results for this calculated: 1.287 Å, 2936 cm^{-1} (32 km/mol). [b] Angle HN−H: 110.9°, dipole moment 5.45 D. HCl results: 1.293 Å, 2894 cm^{-1} (29 km/mol). [c] Angle HN−H: 111.1°, dipole moment 4.93 D. HF results: 0.922 Å, 4101 cm^{-1} (130 km/mol). [d] Angle HN−H: 111.6°, dipole moment 5.05 D. HF results: 0.929 Å, 3995 cm^{-1} (109 km/mol).

TABLE 6: Calculated Effect of Stepwise Decrease in Fixed H_3N-HCl Distance on the B3LYP/6-311+G Optimized Potential Surface**

distances (Å)			frequencies (cm^{-1})				
H−N	N−HCl	H−Cl	H−Cl str	sym NH_3	H−Cl lib	N−HCl str	energy (kcal/mol)
1.0159	1.7235	1.3505	2123	1121	855	195	0.00
1.0161	1.65[a]	1.3653	1944	1137	918	215[a]	+0.08
1.0163	1.60[a]	1.3780	1807	1149	968	229[a]	+0.20
1.0164	1.55[a]	1.3925	1661	1157	1015	243[a]	+0.45
1.0166	1.50[a]	1.4091	1507	1168	1065	260[a]	+0.76
1.0168	1.45[a]	1.4309	1337	1170	1117	276[a]	+1.2
1.0168	1.40[a]	1.4582	1067	1232	1174	295[a]	+1.6
1.0177	1.35[a]	1.4879	920	1236	1232	338[a]	+2.1
1.0173	1.30[a]	1.523	774	1256	1287	415[a]	+2.7

[a] Fixed N−HCl distance: N−HCl stretching mode not rigorous.

bands become stronger relative to the former four-band set with increasing reagent concentration. Hence, the new four-band set is assigned to the 1:1 H_3N-HCl complex.

The strong, sharp 1060.2 cm^{-1} band shifts by 5.4 cm^{-1} to 1054.8 cm^{-1} with $^{15}NH_3$, slightly more than the 4.1 cm^{-1} shift observed for the symmetric bending mode of ammonia itself (968.2 cm^{-1} in neon). On the other hand, ND_3 shifts the band to 824.5 cm^{-1}, which gives a larger frequency ratio (1.286) than observed for ammonia (1.262). Hence, the 1060.2 cm^{-1} band is due to the symmetric NH_3 bending mode in the H_3N-HCl complex with slightly more N and less H involvement than found for isolated NH_3. A quartet of similar bands was observed for both ammonia and the product complex using $^{15}NH_nD_{3-n}$, which indicates that this motion involves the NH_3 subunit with three equivalent hydrogen atoms. The larger shift with $^{15}ND_3$, 7.4 cm^{-1}, is in accord with more nitrogen motion against three deuterium atoms than three hydrogen atoms.

The sharp, weaker 2017.4 cm^{-1} band is due to the first overtone of the 1060.2 cm^{-1} fundamental. This band shifts 9.0 cm^{-1} with $^{15}NH_3$, just less than $2 \times 5.4 = 10.8$ cm^{-1}, because of Fermi resonance and mode mixing with the 2084 cm^{-1} band. The ND_3 counterpart is a characteristic Fermi resonance (FR) window at 1595 cm^{-1} in the broad 1600 cm^{-1} band because of the D−Cl stretching mode in the complex. This window shifts to 1583 cm^{-1} for $^{15}ND_3$, again slightly less than double the shift for the fundamental because of the FR interaction.

The characteristic strong, broad 2084 cm^{-1} band is assigned to the H−Cl fundamental in the H_3N-HCl complex. The 2084 cm^{-1} band shifts to 2079 cm^{-1} with $^{15}NH_3$, and the broad deuterium counterparts at 1600 and 1595 cm^{-1} show a similar 5 cm^{-1} shift with ^{15}N substitution. The observation of FR interaction between the 2084 cm^{-1} fundamental and 2017.4 cm^{-1} overtone in the spectrum of H_3N-HCl and between the two corresponding modes in the D_3N-DCl complex as evidenced by the FR window clearly demonstrates that the broad 2084 cm^{-1} HCl submolecule absorption belongs to the same complex as the sharp 1060.2 cm^{-1} NH_3 submolecule absorption. The H/D ratio 1.303 indicates considerable anharmonicity. The ^{15}N shift observed for the H−Cl and D−Cl stretching modes suggests some coupling with the low-frequency H_3N-HCl hydrogen bond stretching mode, a common occurrence in strong hydrogen-bonded complexes.[39]

The sharp, weaker 708.9 cm^{-1} band exhibits a 698.3 cm^{-1} splitting and no shift with ^{15}N substitution. The 526.1 cm^{-1} deuterium counterpart follows suit with a site splitting and no ^{15}N shift. The 708.9 cm^{-1} band has a characteristic H/D ratio of 1.348 and is assigned to the H−Cl librational mode in the

H_3N-HCl complex. The analogous mode for the $CH_3CN-HCl$ complex at 414 cm^{-1} in solid argon has a 1.380 ratio,[40] but the librational mode for HF in the H_3N-HF complex at 916 cm^{-1} has a 1.315 H/D ratio.[23]

The 2084 cm^{-1} H−Cl fundamental for the H_3N-HCl complex is considerably lower than those for HCl in solid neon (2871 cm^{-1}) and $CH_3CN-HCl$ in solid neon (2676.0 cm^{-1}),[40,41] but much higher than the previously observed hydrogen stretching fundamental for the H_3N-HCl complex in solid argon (1371 cm^{-1}).[7,34]

Argon. The major bands that evolve for the 1:1 H_3N-HCl complex at 1370.9, 1290.3, 1070.0, and 733.9 cm^{-1} using neon/argon mixtures and pure argon hosts at 4−5 K agree with early and recent argon matrix work.[7,34] Additional, new information to help characterize these vibrational modes is found in the $^{15}NH_3$ and relatively pure ND_3 and $^{15}ND_3$ isotopic spectra reported here.

The strong, sharp 1070.0 cm^{-1} absorption shifts to 1064.4 cm^{-1} with $^{15}NH_3$, while ND_3 shifts the band to 831.4 cm^{-1} and $^{15}ND_3$ to 823.7 cm^{-1}. The H/D ratios, 1.287 and 1.292, for the ^{14}N and ^{15}N species are essentially the same as for the corresponding neon matrix bands, and the 1070.0 cm^{-1} band is clearly due to the symmetric NH_3 bending mode in the complex as assigned previously.[7,42] The further 9.8 cm^{-1} *blue shift* in this mode from neon (1060.2 cm^{-1}) to argon (1070.0 cm^{-1}) above the ammonia fundamental suggests a stronger interaction within the H_3N-HCl complex in the argon host than in neon.

The weaker 733.8 cm^{-1} band shows no $^{15}NH_3$ displacement but shifts to 544.0 cm^{-1} with DCl and gives the H/D ratio 1.349, which is almost the same as found in solid neon. This band was assigned earlier to the NH_3 rocking mode,[7] but the lack of $^{15}NH_3$ shift and the band position argue for assignment to the H−Cl librational mode. Note that the increase from 708.9 cm^{-1} in solid neon to 733.8 cm^{-1} in solid argon for this H−Cl librational mode also points to a stronger interaction within the 1:1 complex in the argon host.

The 1370.9 and 1290.3 cm^{-1} absorptions were originally assigned to antisymmetric N−H−Cl stretching and bending modes in the $H_3N-H-Cl$ complex.[7] The new $^{15}NH_3$ data support the stretching mode assignment for the 1370.9 cm^{-1} band, but suggest revising the 1290.3 cm^{-1} band assignment to the first overtone of the H−Cl librational mode. The small $^{15}NH_3$ shift (0.2 cm^{-1}) for the 1290.3 cm^{-1} band may arise from weak FR interaction with the 1370.9 cm^{-1} band, which has a surprisingly large (6.6 cm^{-1}) $^{15}NH_3$ shift. This large 6.6 cm^{-1} shift further underscores the participation of N in the 1370.9 cm^{-1} N−H−Cl vibrational mode, which is probably coupled with the low-frequency symmetric N−H−Cl stretching mode. The deuterium shifts of these bands to 1114.3 and 991.8 cm^{-1} and $^{15}ND_4Cl$ shifts to 1111.0 and 989.8 cm^{-1} are in accord with these mode descriptions; however, there is more interaction between the $D_3N-D-Cl$ stretching and bending overtone modes (based on ^{15}N shifts) than in $H_3N-H-Cl$. The low isotopic ratio 1370.9/1114.3 = 1.230 indicates strong anharmonicity in the potential describing of the proton motion in the hydrogen bond. Model calculations[43] of the effect of mechanical anharmonicity on the H/D isotopic frequency ratio for the hydrogen stretching modes showed that the ratio changes from 1.41 to near 1 with an increase of anharmonicity in the potential function, which agree with reported experimental values.[44] Recent DFT calculations[45] performed for the ammonia−hydrogen chloride complex resulted in an H/D isotopic ratio of 1.27 for the anharmonic proton stretching vibration.

However, interaction between the $D_3N-D-Cl$ antisymmetric stretching mode and an overtone of the HCl librational mode (which forces the 1114.3 cm^{-1} band higher and the resulting 1370.0/1114.3 ratio lower) may also contribute to the low value of the isotopic ratio. It has been shown for hydrogen halide−pyridine derivative complexes with proton-shared N···H···Cl hydrogen bonds that the complicated spectral pattern observed for these complexes in the low-frequency region arises from normal coordinate mixing of proton motion with internal motions of the complexes.[46,47] Such normal coordinate mixing probably contributes to the spectra of the ammonia−hydrogen chloride complex.

The 3429.9 cm^{-1} band and isotopic counterparts track with the 1:1 absorptions on annealing and are assigned to the ν_3 (e) ammonia mode in the H_3N-HCl complex.

In conclusion, the substantial red shift in the H−Cl stretching mode from solid neon (2084 cm^{-1}) to the 1370.9 cm^{-1} antisymmetric N−H−Cl stretching mode in solid argon arises from the increased H_3N-HCl interaction, which is also manifested in the blue shifts in the symmetric NH_3 bending and H−Cl librational modes going from neon to argon hosts.

Krypton. We discovered that krypton with 10% neon added forms an effective, transparent matrix at 4−5 K, and that successive annealing to 22, 30, 40, and 50 K allows controlled sublimation of neon with diffusion and association of trapped HCl and NH_3 in the solid krypton matrix. Figure 6 illustrates the growth of 1281.3, 1272.4, 1218.6, 1071.9, and 733.9 cm^{-1} absorptions on annealing to 40 K followed by their decrease in concert on annealing to 50 K; the 1388.5 cm^{-1} band appears to be due to a different species, and the above bands are assigned to the 1:1 complex. The 1281.3 and 1218.6 cm^{-1} bands decreased almost 3 cm^{-1} on annealing to 40 K, and the 1071.9 cm^{-1} band increased 0.3 cm^{-1} as the neon sublimed from the krypton host, but these positions did not change on the final 50 K annealing, which decreased the band absorbances. We conclude that the remaining host is now pure krypton and that the frequencies reflect this environment as shown in a pure krypton experiment.

The straightforward assignments of the 1071.9 and 736.9 cm^{-1} bands to the symmetric NH_3 bending and H−Cl librational modes in the H_3N-HCl complex follow their positions in solid argon and similar isotopic shifts in solid krypton. Note that the blue shifts in these two modes going from solid argon (1070.0, 733.8 cm^{-1}) to solid krypton indicate a slightly stronger hydrogen-bonding interaction in the krypton matrix.

The counterparts of the 1281.3 cm^{-1} band in ND_4Cl, $^{15}ND_4Cl$ experiments were identified at 991.4, 988.9 cm^{-1}, and the counterparts of the 1218.6 cm^{-1} absorption were observed at 911.4, 904.6 cm^{-1}, respectively. Such correlation is suggested by similar ^{15}N isotopic shifts for the 1281.3, 991.4 cm^{-1} bands (1.6, 2.5 cm^{-1}) and 1218.6, 911.4 cm^{-1} bands (8.3, 6.8 cm^{-1}) in hydrogen and deuterium experiments. No deuterium counterpart was found for the1272.4 cm^{-1} band. The frequencies of the 1281.3 cm^{-1} band and its counterparts in krypton experiments (1281.3, 1279.7, 991.4, 988.9 cm^{-1}) are very close to the frequencies of the 1290.3 cm^{-1} band and its counterparts in argon experiments (1290.3, 1290.1, 991.8, 989.8 cm^{-1}), which suggest that the corresponding absorptions are due to the same mode, namely the first overtone of the H−Cl librational mode. The 1218.6 cm^{-1} absorption shows a relatively large ^{15}N shift like the 1370.9 cm^{-1} band in the argon experiment and is assigned, accordingly, to the antisymmetric N−H−Cl stretching mode. Assignment of the 1272.4 cm^{-1} absorption is not clear. However, one has to remember that in this low-frequency region,

the normal modes are strongly mixed, and proton motion probably contributes to the other modes observed in this region. This fact may account for the relatively large intensity of the 1281.3 cm^{-1} band and its counterparts.

The substantial red shift of the antisymmetric N−H−Cl stretching mode from argon (1370.9 cm^{-1}) to krypton (1218.6 cm^{-1}) follows the blue shift of the symmetric NH_3 bending and H−Cl librational modes from argon to krypton (1070.0 to 1071.9 cm^{-1} and 733.8 to 736.9 cm^{-1}, respectively) and indicates that the krypton matrix strenghtens the hydrogen bond in the ammonia−hydrogen chloride complex as compared to the argon matrix.

Neon/Argon. The spectra of neon/argon mixtures (Figure 4) show that the 1:1 complex in solid neon (Figure 1) evolves to the 1:1 complex in solid argon (Figure 5), and that the same 1:1 H_3N−HCl complex is observed in both matrix hosts. It is clear that the 2084 cm^{-1} band is most sensitive to the effect of argon replacing neon in the surrounding sphere of matrix atoms from the red shift observed, but a steady increase in the strong 1060.2 cm^{-1} band (neon) to the 1070.0 cm^{-1} band (argon) is also observed on increasing the percent argon and on annealing to allow diffusion, where argon clearly replaces neon in the intimate influential matrix layer. The 1:1 complex is large enough to require a two-matrix atom vacancy, and the immediate surrounding layer will contain at least 12 matrix atoms. First, the spectra reveal many band positions for the H−Cl vibration in the H_3N−HCl complex between the pure neon (2084 cm^{-1}) and pure argon (1371 cm^{-1}) values. Even with 1% argon in neon, the new peak shifts to 2079 cm^{-1} and then further to 2061 cm^{-1} on annealing as Ar replaces Ne in critical positions in the solvation shell. With 5% Ar in Ne (Figure 4), the major absorption at 2045 cm^{-1} shifts to 2015, 1970, and 1935 cm^{-1} on successive annealing to 8, 10, and 12 K, while a new, broad band appears at 1420 cm^{-1}. In addition, the higher band shifts to 1920 and 1910 cm^{-1} with 10% and 25% argon, while the lower band shifts to 1385 and 1372 cm^{-1}. The discontinuity (between 1910 and 1420 cm^{-1}) implies that some sites in the solvation shell are more important than others and that cavity size may change abruptly. The cavity size is, of course, part of the "matrix effect" in addition to the electrostatic solvation. Furthermore, the H−Cl band positions in solid Ne, Ar, and Kr (2084, 1371, and 1218 cm^{-1}) do not follow directly the permittivities of these noble gases (1.24, 1.63, and 1.88), which provide further evidence that cavity size may also be an important factor. The bottom line here is that the argon matrix effect on H_3N−HCl is substantial, and there is much more H−Cl bond elongation and a much lower H−Cl frequency in solid argon than in solid neon.

As the argon percent is increased, the neon 1060.2 cm^{-1} frequency increases continuously to the argon 1070.0 cm^{-1} value, while the neon 2084 cm^{-1} frequency decreases to about 1910 cm^{-1}, and then reappears at 1420 cm^{-1} before falling to the argon 1371 cm^{-1} value. The H−Cl mode may depend more particularly on the matrix atoms surrounding the HCl submolecule in the complex, but attempts to model the matrix effect using three atoms do not account for the large shift observed.[20]

Nitrogen. The 1438, 1246, 705, and 630 cm^{-1} bands first assigned to the 1:1 H_3N−HCl complex by Ault and Pimentel[6] can be further analyzed with the $^{15}NH_3$ spectra observed here. Our NH_4Cl decomposition experiments gave considerably lower reagent concentrations, and little aggregation, and the sharper product absorptions were measured at 3419.7, 1443.9, 1251.6, 702, and 628 cm^{-1} with $^{14}NH_4Cl$ and at 3411.4, 1438.4, 1245.5, 700, and 625 cm^{-1} with $^{15}NH_4Cl$. Annealing shows that additional 750 cm^{-1} and split 1115.8, 1106.0 cm^{-1} absorptions are due to higher complexes: the latter sharp bands, also reported by Barnes et al.,[7] show a large 5.1 cm^{-1} nitrogen isotopic shift, which describes a perturbed symmetric NH_3 bending mode. The sharp 1415.0 cm^{-1} band is observed *before* any absorption near 3100 cm^{-1}, and it grows on annealing *before* being engulfed by the stronger 1405.0 cm^{-1} absorption and associated bands at 3141.7, 3058.0, and 1794.9 cm^{-1}. The latter are due to $NH_4^+Cl^-$ in sufficient cluster size to approach the solid spectrum; the weaker 1794.9 cm^{-1} absorption is a combination band involving the NH_4^+ ion ν_4 fundamental and a torsional lattice mode;[36] note that the $(\nu_4 + \nu_6) - (\nu_4)$ differences 389.9 and 389.8 cm^{-1} show no ^{15}N shift within experimental error and agree with the frequency inferred (391 cm^{-1}) from the solid spectrum.[36] The $NH_4^+Cl^-$ bands shifted only slightly (3125, 3054, 1403 cm^{-1}) after the matrix was evaporated at 70 K, and the window recooled to 5 K. The sharp 1415.0 cm^{-1} band is probably due to a small $(NH_4^+)_x(Cl^-)_y$ cluster analogous to the sharp 1418.0 cm^{-1} neon matrix band.

Barnes et al.[7] argue convincingly that the 1246 cm^{-1} band for H_3N−HCl is an ammonia submolecule mode and not a N···H···Cl overtone as first assigned,[6] and they offer a 1096 cm^{-1} D_3N−HCl counterpart and a 999 cm^{-1} D_3N−DCl component. The present ^{15}N shift for the former band, 6.1 cm^{-1}, supports the ammonia (a_1) mode characterization. Barnes et al. reassign the band near 630 cm^{-1} to a NH_3 rocking mode; however, our DFT calculations predict the weak rocking mode much lower and the bending (or librational) mode much higher (Table 6); the bending mode is probably overestimated by the DFT calculation. The band observed here at 702.5 ± 0.5 cm^{-1} is due to the antisymmetric N···H···Cl stretching mode in agreement with both previous groups:[6,7] the 2 cm^{-1} ^{15}N shift agrees with this assignment. The 3419.7 cm^{-1} absorption showed a large 8.3 cm^{-1} ^{15}N shift, which is appropriate for the antisymmetric H_3−N stretching mode in the complex. In agreement with previous work,[6,7,18] the proton is apparently shared as H_3N···H···Cl *in the more strongly interacting nitrogen matrix*, which is supported by the strong fundamental for $(Cl-H-Cl)^-$ at 696 cm^{-1}.[52]

Note that the 1251.6 cm^{-1} nitrogen matrix frequency for NH_3 in H_3N···H···Cl is much higher than the 1070.0 and 1060.2 cm^{-1} argon and neon matrix values for H_3N−HCl, which represent less severe perturbations on NH_3. As a proton attaches to NH_3 to become NH_4^+, the NH_3 modes at 1630 cm^{-1} (e) and 970 cm^{-1} (a_1) become (t_2) near 1405 cm^{-1}. The H_3N···H···Cl complex in nitrogen is an intermediate case with 1443.9 cm^{-1} (e) and 1251.6 cm^{-1} (a_1) modes. Accordingly, the 1443.9 cm^{-1} band is characterized as an NH_3 (e) mode, and the 5.5 cm^{-1} ^{15}N shift supports this reassignment.

Calculations. The DFT calculations predict HCl and HF bond lengths slightly longer than experimental values, but the B3LYP results are only 0.005 Å longer (Table 5). Harmonic frequency predictions are below the experimental values but near the observed anharmonic frequencies, with B3LYP slightly higher than BPW91, as found previously.[48] However, the DFT calculations predict the crucial diagnostic N···X bond lengths in the H_3N−HX complexes 2−4% shorter than the gas-phase measurements,[11,38] with the B3LYP functional giving closer agreement. Accordingly, we may expect reasonable predictions of approximate frequencies as support for vibrational assignments with the B3LYP functional giving better agreement.

The H_3N−HF complex has been examined in the gas phase and the H−F fundamental measured[22] at 3215 cm^{-1}; our B3LYP frequency (3260 cm^{-1}) is 1.4% high and BPW91 frequency

(3023 cm^{-1}) is 6.0% low. This is the order expected for these functionals,[48] but there is no database for comparison with observed values for such complexes. In the neon matrix, the H−F fundamental is 3106 cm^{-1}, a 109 cm^{-1} red shift, the symmetric NH_3 bend 1090 cm^{-1}, and the H−F libration 912 cm^{-1} for the H_3N−HF complex.[21] Table 5 shows that the B3LYP values are slightly higher but in generally good agreement. These harmonic DFT frequencies are not expected to be a perfect model, but they provide support for the experimental assignments. In this regard, the harmonic MP2 calculation[20] for H_3N−HF predicted a harmonic H−F frequency of 3296 cm^{-1}, higher than our B3LYP value, and gave one- and two-dimensional anharmonic frequencies at 2949 and 2832 cm^{-1}, which are much lower than the gas-phase 3215 cm^{-1} value. This MP2 calculation *overestimates* the anharmonicity in the H−F stretching mode.

Based on the calculated N···Cl bond length, our B3LYP calculation slightly overestimates the strength of the H_3N−HCl interaction (bond 0.063 Å shorter), and the BPW91 calculation overestimates this interaction even more (bond 0.117 Å shorter). The computed HCl frequencies follow this trend: the B3LYP values for the very strong H−Cl stretching mode (2123 cm^{-1}) and H−Cl libration (855 cm^{-1}) change to 1901 and 922 cm^{-1}, respectively, with BPW91 (Table 4). However, the B3LYP predictions, including the symmetric NH_3 mode (1121 cm^{-1}), are clearly in reasonable agreement with the neon matrix values (2084, 1060, 709 cm^{-1}), but the hydrogen-bonding interaction is overestimated at the B3LYP level based on these three diagnostic observed frequencies. Note also that the calculated hydrogen bond-stretching mode (195 cm^{-1}) is slightly higher than the microwave and argon matrix values (160 ± 2 and 166 cm^{-1}).[7,11] Even though the present B3LYP frequency calculation for the H_3N−HCl complex is only a crude approximation, it provides support for the neon matrix assignments to H_3N−HCl as representative of the gas-phase complex and shows that the argon matrix spectrum is a direct consequence of a stronger matrix interaction with the complex, which increases the hydrogen bonding effect. This conclusion agrees with a recent discussion of Barnes and Legon.[18]

The H_3N−HCl potential surface has been explored with artificially increased proton transfer to match the effect of matrix solvation by stepwise decrease of a fixed N···H distance, followed by optimization of the other structural parameters and calculation of the frequencies that characterize this stronger interaction. This stepwise decrease of the hydrogen bond distance from the optimized 1.7235 Å value to 1.30 Å leads to a small 2.7 kcal/mol increase in the energy, which indicates that the computed structures are near the global energy minimum. Although the calculated N−HCl stretching mode is small, it is not rigorous nor physically meaningful, but the predicted trends in H−Cl stretching and symmetric NH_3 bending modes, summarized in Table 6, are reasonable. For a N···HCl distance of 1.50 Å, the H−Cl frequency (1507 cm^{-1}) approximates the argon matrix value, but the increase in the symmetric NH_3 mode (47 cm^{-1}) exceeds considerably the 10 cm^{-1} neon−argon shift, as does the increase in the H−Cl librational mode. However, the energy increase, 0.76 kcal/mol, is reasonable for argon solvation. For a N···HCl distance of 1.30 Å, the N−H−Cl frequency (779 cm^{-1}) and symmetric NH_3 mode (1252 cm^{-1}) approximate the nitrogen matrix values.

A calculation was done for $(HCl)_2$ to predict relative infrared intensities. The B3LYP/6-311+G** calculation gave 2929 cm^{-1} (42 km/mol) and 2874 cm^{-1} (215 km/mol) frequencies for H−Cl stretching modes, which may be compared to HCl (2936 cm^{-1}, 32 km/mol) and the gas-phase $(HCl)_2$ dimer fundamentals at 2880 and 2839 cm^{-1}.[49] Therefore, the dominance of HCl monomer over $(HCl)_2$ dimer in our matrix spectra is approximately 7 times more than the relative band absorbances.

TABLE 7: Frequencies (cm^{-1}) Assigned to Ammonia−HF and Ammonia−HCl Complexes in Solid Neon, Argon, and Krypton

complex	H−X str	sym NH_3 bend	H−X lib
H_3N−HF in Ne[a]	3106	1090	912
H_3N−HF in Ar[b]	3041	1093	916
H_3N−HCl in Ne	2084	1060	709
H_3N−HCl in Ar	1371	1070	734
H_3N−HCl in Kr	1218	1072	737

[a] Reference 21. [b] Reference 23.

A final comparison with the MP2 calculations for H_3N−HCl is in order. First, the harmonic MP2 frequency for HCl in the complex (2528 or 2541 cm^{-1})[15a,19] is considerably higher than our B3LYP value, our neon matrix value (2084 cm^{-1}), and our 2200 cm^{-1} estimated extrapolation to the gas-phase value. The MP2 one-dimensional anharmonic frequency (2278 cm^{-1}) is reasonable, but the two-dimensional prediction (1869 cm^{-1})[19] substantially overestimates the anharmonic correction needed for the H_3N−HCl complex in the gas phase.

Matrix-to-Gas Shifts. A major reason to examine the neon matrix spectrum of the H_3N−HCl complex is to extrapolate to the gas-phase frequency. Legon describes the nature of gaseous H_3N−HCl in the ground vibrational state as a traditional (simple) molecular complex ("no substantial proton transfer") on the basis of Cl nuclear quadrupole coupling constants and intermolecular stretching force constants, based on the centrifugal distortion model.[11] These quantities are about 10% of the way between HCN···HCl (traditional, simple molecular) and Na^+Cl^- (representing the ionic, proton-transferred form). Hence, a simple hydrogen-bonded model H_3N−HCl with only polarization of HCl by the NH_3 unit and a small extension of the H−Cl bond are invoked. The microwave spectrum suggests a small extension of the H−Cl bond, although the N···Cl distance (3.137 Å) is shorter than in other complexes (CH_3CN−HCl, 3.301 Å, for example).[11,50] However, the infrared spectrum also interrogates the $v = 1$ level, where anharmonicity will be more important. For the CH_3CN−HCl complex, the gas-phase, neon matrix, and argon matrix H−Cl frequencies are 2714 ± 3, 2676, and 2662 cm^{-1}, respectively.[40,41,51] However, for the more strongly hydrogen-bonded H_3N−HCl complex, the argon perturbation is substantial, and the neon matrix 2084 cm^{-1} observation points to a higher gas-phase band position estimated to be near 2200 cm^{-1}. Table 7 compares the H−F fundamental in the similar H_3N−HF complex for neon (3106 cm^{-1}) and argon matrix (3041 cm^{-1}) hosts, which are slightly lower than the 3215 cm^{-1} gas-phase value. The stronger argon matrix interaction stabilizes the complex, red shifts the H−F stretching mode, and blue shifts the symmetric NH_3 bending and H−F librational modes relative to the neon matrix values.

The same behavior is found for the H_3N−HCl complex, but we have Ne, Ar, and Kr matrix hosts to contrast. The more polarizable host clearly stabilizes the complex and increases the perturbation on the submolecule mode (the HX libration is a rotation for isolated HX). The argon value for the H−Cl libration is 89% of the blue shift between neon and krypton values, and the argon position of the symmetric NH_3 mode is 83% of the neon−krypton blue shift, whereas the argon matrix H−Cl stretch is 82% of the red shift from neon to krypton. These displacements are all internally consistent, and they support the polarizable solvent stabilization of the hydrogen-bonding in-

teraction with increasing H−Cl bond length and decreasing N−H hydrogen bond length in the H_3N−HCl complex. This trend is continued in the nitrogen matrix, where an intermediate case H_3N···H···Cl is characterized by a still lower N···H···Cl stretching mode and a still higher symmetric NH_3 bending mode.

Vibrational spectra are more complicated than ground-state spectra as the $v = 1$ level is also involved, and the $v = 1$ state has more H−Cl elongation, "proton transfer," and anharmonicity, and accordingly, more interaction with the matrix host. We simply wish to point out that interaction of the $v = 1$ state with the neon matrix results in a much smaller matrix effect (probable red shift from the gas-phase $v = 0 \rightarrow v = 1$ transition) than interaction with the argon and krypton matrices. Theoretical attempts[19] to model the argon matrix interaction with three argon atoms, even with a one-dimensional anharmonic model, fail to account for the magnitude of the observed argon matrix frequency (1371 cm^{-1}). However, the inclusion of reasonable electric fields[20] with the anharmonic model does account for the argon matrix frequency.

Finally, an experiment with the still less polarizable D_2 matrix was performed. Even though HCl and $(HCl)_2$ gave sharp absorptions, the small cage apparently does not allow for rotation of HCl. The H_3N−HCl complex is apparently too large to be trapped in a unique site in solid D_2, and the broad 1054 cm^{-1} band for the NH_3 submolecule mode resulted. Nevertheless, this mode is blue shifted less (72 cm^{-1}) in solid D_2 compared to that in solid Ne (92 cm^{-1}), indicating a weaker interaction with the D_2 matrix host.

Conclusions

Ammonia and hydrogen chloride vapors from thermal decomposition of NH_4Cl co-deposited with excess neon at 4−5 K formed the H_3N−HCl complex. Strong, broad 2084 cm^{-1} and strong, sharp 1060.2 cm^{-1} absorptions are assigned to the H−Cl stretching and symmetric NH_3 bending modes and weaker 2017.4 and 708.9 cm^{-1} bands to the overtone of the NH_3 mode and the H−Cl librational fundamental of the 1:1 complex, respectively. Vibrational assignments are supported by $^{15}NH_4Cl$, ND_4Cl, and $^{15}ND_4Cl$ isotopic substitution. To our knowledge, this is the first observation of Fermi resonance between modes of the two submolecules in a hydrogen-bonded complex, which underscores the strong coupling of normal modes in the H_3N−HCl complex. Simple B3LYP/6-311+G** density functional calculations reproduce these three fundamental frequencies reasonably well and support the assignment of the neon matrix spectrum to the H_3N−HCl complex with only slight matrix perturbation.

Complementary experiments were done with neon/argon mixtures, argon, krypton, and nitrogen to investigate the 1:1 complex in a range of matrix environments. The evolution of the neon matrix spectrum with argon dilution to the argon matrix spectrum shows that the same 1:1 complex is isolated in each host. The neon matrix spectrum suggests a strong hydrogen bond, with slightly more H−Cl elongation than in the gas-phase complex based on the microwave spectrum of the $v = 0$ state complex,[11] but not as much as found in the argon, krypton, and nitrogen matrix hosts. Clearly, matrix interaction will be larger for the $v = 1$ state than the $v = 0$ state, which affects the infrared spectrum. Even in solid argon and krypton, the proton is not shared evenly, as the H−Cl stretching frequencies are still far above the $(Cl-H-Cl)^-$ value (696 cm^{-1} in solid argon);[52] however, in solid nitrogen, proton sharing appears to be approached (702 cm^{-1} mode).[6,7,18]

Acknowledgment. We acknowledge financial support from the National Science and Kosciuszko Foundations and the friendly and helpful exchange of information with W. B. Person and K. Szczepaniak before publication.

References and Notes

(1) Legon, A. C. *Chem. Soc. Rev.* **1993**, 153 and references therein.
(2) Clementi, E. *J. Chem. Phys.* **1967**, *46*, 3851; *47*, 2323.
(3) Goldfinger, P.; Verhaegen, G. *J. Chem. Phys.* **1969**, *50*, 1467.
(4) Shibata, S. *Acta Chem. Scand.* **1970**, *24*, 705.
(5) Jones, W. J.; Seel, R. M.; Sheppard, N. *Spectrochim. Acta* **1969,** *25A*, 385.
(6) Ault, B. S.; Pimentel, G. C. *J. Phys. Chem.* **1973**, *77*, 1649.
(7) Barnes, A. J.; Beech, T. J.; Mielke, Z. *J. Chem. Soc., Faraday Trans. 2* **1984**, *80*, 455.
(8) Barnes, A. J.; Kuzniarski, J. N. S.; Mielke, Z. *J. Chem. Soc., Faraday Trans. 2* **1984**, *80*, 465.
(9) Barnes, A. J.; Wright, M. P. *J. Chem. Soc., Faraday Trans. 2* **1986**, *82*, 153.
(10) Schriver, L.; Schriver, J.; Perchard, J. P. *J. Am. Chem. Soc.* **1983**, *105*, 3843.
(11) Howard, N. W.; Legon, A. C. *J. Chem. Phys.* **1988**, *88*, 4694.
(12) Latajka, Z.; Sakai, S.; Morokuma, K.; Ratajczak, H. *Chem. Phys Lett.* **1984**, *110*, 464. Latajka, Z.; Scheiner, S.; Ratajczak, H. *Chem. Phys Lett.* **1987**, *135*, 367.
(13) Latajka, Z.; Scheiner, S. *J. Chem. Phys.* **1984**, *81*, 4014.
(14) Brciz, A.; Karpfen, A.; Lischka, H.; Schuster, P. *Chem. Phys.* **1984**, *89*, 337.
(15) (a) Cazar, R. A.; Jamaka, A. J.; Tao, F.-M. *J. Phys. Chem. A* **1998**, *102*, 5117. (b) Pursell, C. J.; Zaidi, M.; Thompson, A.; Fraser- Gaston, C.; Vela, E. *J. Phys.* **2000**, *104*, 552.
(16) Seinfeld, J. H. *Atmospheric Chemistry and Physics of Air Pollution*; Wiley: New York, 1986.
(17) Tao, F.-M. *J. Chem. Phys.* **1999**, *110*, 11121.
(18) Barnes, A. J.; Legon, A. C. *J. Mol. Struct.* **1998**, *448*, 101.
(19) Del Bene, J. E.; Jordan, M. J. T. *J. Chem. Phys.* **1998**, *108*, 3205.
(20) Jordan, M. J. T.; Del Bene, J. E. *J. Am. Chem. Soc.* **2000**, *122*, 2101.
(21) Andrews, L. In *Chemistry and Physics of Matrix Isolated Species*; Andrews, L., Moskovits, M., Eds.; Elsevier: Amsterdam, 1989; Chapter 2.
(22) Thomas, R. K. 3215 cm^{-1} absorption for H−F mode in H_3N−HF complex, unpublished work, communicated to the corresponding author in 1981.
(23) Johnson, G. L.; Andrews, L. *J. Am. Chem. Soc.* **1982**, *104*, 3043.
(24) Andrews, L.; Wang, X.; Mielke, Z. *J. Am. Chem. Soc.* **2001**, *123*, 1499.
(25) Vapor pressure 2 to 10 mTorr: *Handbook of Chemistry and Physics*; Chemical Rubber Co. Publishing: Cleveland, OH, 1968; D-139.
(26) Abouaf-Marquin, L.; Jacox, M. E.; Milligan, D. E. *J. Mol. Spectrosc.* **1977**, *67*, 34.
(27) Frisch, M. J.; Trucks, G. W.; Schlegel, H. B.; Scuseria, G. E.; Robb, M. A.; Cheeseman, J. R.; Zakrzewski, V. G.; Montgomery, J. A., Jr.; Stratmann, R. E.; Burant, J. C.; Dapprich, S.; Millam, J. M.; Daniels, A. D.; Kudin, K. N.; Strain, M. C.; Farkas, O.; Tomasi, J.; Barone, V.; Cossi, M.; Cammi, R.; Mennucci, B.; Pomelli, C.; Adamo, C.; Clifford, S.; Ochterski, J.; Petersson, G. A.; Ayala, P. Y.; Cui, Q.; Morokuma, K.; Malick, D. K.; Rabuck, A. D.; Raghavachari, K.; Foresman, J. B.; Cioslowski, J.; Ortiz, J. V.; Baboul, A. G.; Stefanov, B. B.; Liu, G.; Liashenko, A.; Piskorz, P.; Komaromi, I.; Gomperts, R.; Martin, R. L.; Fox, D. J.; Keith, T.; Al-Laham, M. A.; Peng, C. Y.; Nanayakkara, A.; Gonzalez, C.; Challacombe, M.; Gill, P. M. W.; Johnson, B.; Chen, W.; Wong, M. W.; Andres, J. L.; Gonzalez, C.; Head-Gordon, M.; Replogle, E. S.; Pople, J. A. *Gaussian 98*, Revision A.7; Gaussian, Inc.: Pittsburgh, PA, 1998.
(28) (a) Becke, A. D. *Phys. Rev. A* **1988**, *38*, 3098. (b) Perdew, J. P.; Wang, Y. *Phys. Rev. B* **1992**, *45*, 13244.
(29) (a) Becke, A. D. *J. Chem. Phys.* **1993**, *98*, 5648. (b) Lee, C.; Yang, W.; Parr, R. G. *Phys. Rev. B* **1988**, *37*, 785.
(30) (a) Krishnan, R.; Binkley, J. S.; Seeger, R.; Pople, J. A. *J. Chem. Phys.* **1980**, *72*, 650. (b) Frisch, M. J.; Pople, J. A.; Binkley, J. S. *J. Chem. Phys.* **1984**, *80*, 3265.
(31) Suzer, S.; Andrews, L. *J. Chem. Phys.* **1987**, *87*, 5131.
(32) Andrews, L.; Bohn, R. B. *J. Chem. Phys.* **1989**, *90*, 5205.
(33) Evans, J. C. *Spectrochim. Acta* **1960**, *16*, 994.
(34) Person, W. B.; Szczepaniak, K. H_3N−HCl in solid argon, to be published.
(35) Maillard, D.; Schriver, A.; Perchard, J. P.; Girardet, C. *J. Chem. Phys.* **1979**, *71*, 505.
(36) Wagner, E. L.; Hornig, D. F. *J. Chem. Phys.* **1950**, *18*, 296. Morgan, H. W.; Staats, P. A.; Goldstein, J. H. *J. Chem. Phys.* **1957**, *27*, 1212.

(37) Huber, K. P.; Herzberg, G. *Constants of Diatomic Molecules*; Van Nostrand Reinhold: New York, 1979.

(38) Clements, V. A.; Langridge-Smith, P. R. R.; Howard, B. J. 2.66 Å N---F bond length for H_3N-HF, unpublished, communicated to the corresponding author in 1981.

(39) (a) Millen, D. J. *J. Mol. Struct.* **1983**, *100*, 351. (b) Legon, A. C.; Millen, D. J. *Chem. Rev.* **1986**, *86*, 635.

(40) The $CH_3CN-HCl$ and $CH_3CN-DCl$ complexes were measured in solid neon at 2676.0 and 1943.1 cm^{-1}, respectively, in this laboratory.

(41) Compare 2662 cm^{-1} in solid argon: Johnson, G. L.; Andrews, L. *J. Phys. Chem.* **1983**, *87*, 1852.

(42) This overtone of the 1070.0 cm^{-1} fundamental was not observed in solid argon, presumably owing to lack of a FR partner in the appropriate region.

(43) Guissani, Y.; Ratajczak, H. *Chem. Phys.* **1981**, *62*, 319.

(44) Novak, A. *Struct. Bonding* **1974**, *18*, 177.

(45) Latajka, Z.; Biczysko, M., to be published.

(46) Del Bene, J. E.; Person, W. B.; Szczepaniak, K. *Chem. Phys. Lett.* **1995**, *247*, 89.

(47) Szczepaniak, K.; Chabrier, P.; Person, W. B.; Del Bene, J. E. *J. Mol. Struct.* **1997**, *367*, 436.

(48) Bytheway, I.; Wong, M. W. *Chem. Phys. Lett.* **1988**, *282*, 219.

(49) Ohashi, N.; Pine, A. S. *J. Chem. Phys.* **1984**, *81*, 73.

(50) Legon, A. C.; Millen, D. J.; North, H. M. *J. Phys. Chem.* **1987**, *91*, 5210.

(51) Thomas, R. K.; Thompson, H. *Proc. R. Soc. London, Ser. A* **1970**, *316*, 303.

(52) Milligan, D. E.; Jacox, M. E. *J. Chem. Phys.* **1970**, *53*, 2034. Wight, C. A.; Ault, B. S.; Andrews, L. *J. Chem. Phys.* **1976**, *65*, 1244.